Technical University of Denmark

Prediction of half harmonic generation in stacked Josephson junctions and Bi2Sr2CaCu2Ox single crystals

Pedersen, Niels Falsig; Sakai, Shigeki

Published in:
Physical Review B (Condensed Matter and Materials Physics)

Link to article, DOI:
10.1103/PhysRevB.61.11328

Publication date:
2000

Document Version
Publisher's PDF, also known as Version of record

Prediction of half harmonic generation in stacked Josephson junctions and $Bi_2Sr_2CaCu_2O_x$ single crystals

Niels Falsig Pedersen
Department of Electric Power Engineering, Technical University of Denmark, DK-2800 Lyngby, Denmark

Shigeki Sakai
Electrotechincal Laboratory, Umezono, Tsukuba, Ibaraki 305-8568, Japan

(Received 10 January 2000)

We demonstrate analytically that parametric excitation of certain plasma resonance modes in $Bi_2Sr_2CaCu_2O_x$ single crystals is possible. The model we use is that of a Josephson stack, and the fundamental mechanism is that of half harmonic generation in time and space when a threshold of the applied rf signal is exceeded. The phenomenon is important as a diagnostic tool for the investigation of plasma resonance in $Bi_2Sr_2CaCu_2O_x$-like materials, as well as being a basis for making high-T_c high-frequency parametric amplifiers. It has some unique features of space and time nonlinear behavior.

The topic of plasma resonance in $Bi_2Sr_2CaCu_2O_x$ (BSCCO) single crystals has recently attracted a lot of interest.[1–9] It is generally agreed that the model for such a system is very similar to that of stacked Josephson junctions. For the theoretical understanding, two different coupling mechanisms for coupling between layers have been proposed, the charge coupling model[2,5–6] and the inductive coupling model.[10,8–9] In this paper we demonstrate analytically and numerically within the framework of the inductive coupling model, that half harmonic generation in stacked Josephson junctions obtained by pumping at a frequency twice the plasma frequency, is possible. The mechanism we investigate here has all the characteristic features of parametric subharmonic generation known from small area Josephson junctions, and thus for example can be utilized to make parametric amplifier at several hundred gigahertz with high impedance. In addition, of course, the observation or nonobservation of such an effect may be used as a diagnostic tool to distinguish between the different models for BSCCO plasma resonance.

In order to derive the equations for parametric half harmonic generation in the anisotropic layered superconductor BSCCO a brief discussion of the stacked Josephson junction plasma resonance in the framework of the inductive coupling model[8,9] is necessary.

In Refs. 8 and 9 it was shown that a system of $(N+1)$-superconducting layers having N coupled Josephson junctions, has N different plasma frequencies, of which only some can be observed with an external rf signal. Among those N different plasma frequencies, one deserves special attention—the so-called in-phase mode plasma frequency. For any number of stacks N, this particular plasma frequency has the highest value among all the possible plasma frequencies, and is characterized by having all N junctions oscillating in phase.[8] This mode was derived analytically for the cases $N=2$, $N=3$ in Ref. 8 and numerically for $N \gg 1$ in Ref. 9. For $N=2$ it was demonstrated that for this mode the voltage of the two junctions were identical and that these voltages had properties very similar to the single junction case. This information will be utilized below in deriving the plasma resonance half harmonic generation for the $N=2$ case. By analogy (and proven by numerical simulation) we will deduce that the phenomenon also exist for large N.

Figure 1 shows a schematic drawing of a stacked Josephson junction. As demonstrated in Ref. 10 the general form of the equations for the stacked Josephson system may be written in the general form

$$\Lambda_J^2 \boldsymbol{\phi}_{xx} = \mathbf{D}(\mathbf{Q} - \mathbf{J}^{-1}\mathbf{I}_B), \tag{1}$$

where $\boldsymbol{\phi}$, $\mathbf{Q}$, and $\mathbf{I}_B$ are vectors whose ith components are the phase difference ϕ_{ii-1}, the dimensionless junction current Q_{ii-1} and the bias current $I_{B,ii-1}$ of the ith junction.

$\mathbf{D}$ is the matrix expressing the inductive coupling, and Λ_J and $\mathbf{J}$ are diagonal matrices for the Josephson penetration length and the maximum Josephson current, respectively. The details of these quantities may be found in Refs. 9 and 10. Here we will specialize to the case of $N=2$ and consider only the in-phase mode defined by $\phi_{10}=\phi_{21}=\phi$. For this case we may write[10]

$$-\phi_{xx}\Gamma^2 + \phi_{tt} + \alpha\phi_t + \sin\phi = \eta_0 + \eta_{\rm rf}\cos(\Omega t - Kx), \tag{2}$$

where x is normalized to the Josephson penetration length for a single junction, $\lambda_J^{(1)} = \sqrt{\hbar/2e\mu_0 d' J}$, time is normalized to

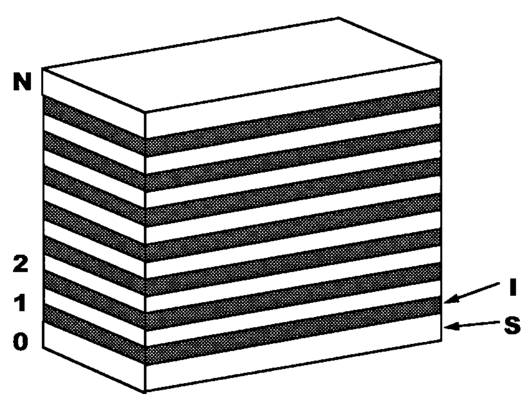

FIG. 1. Schematic drawing of a stacked Josephson junction.

the inverse of the single junction plasma frequency $\omega_0^{-1} = (\hbar C/2eJ)^{-1/2}$, $\alpha = 1/\sqrt{\beta_c}$, where β_c is the McCumber parameter, $\beta_c = 2eR^2CJ/\hbar$. $\Gamma = \lambda_J^{(2)}/\lambda_J^{(1)} = c^{(2)}/c^{(1)} = \sqrt{d'/(d'+s)}$ where the quantities here have their usual meaning,[10] thus the effective thickness $d' = d + \lambda_0 \coth(t_0/\lambda_0) + \lambda_1 \coth(t_1/\lambda_1)$, and the coupling parameter $s = -\lambda_1/\sinh(t_1/\lambda_1)$. $c^{(2)}$ is the inphase light velocity and $c^{(1)}$ is the usual single-junction Swihart velocity, $c^{(2)} > c^{(1)}$, λ_J^2 is the effective two-junction-Josephson penetration depth. The normalized bias current $\eta_0 + \eta_{\mathrm{rf}} \cos(\Omega t - Kx)$ consists of a dc part η_0 and a time-dependent part, which also has a spatial dependence.

The use of an rf current drive term may not always be justified in a long Josephson junction, where in many cases the coupling of rf fields takes place through the edges of the junction, i.e., with boundary conditions in Eq. (2). The use of an rf current term is justified to be able to use the analytical results from small junctions. We have tried numerically to use rf magnetic-field boundary conditions instead and found the half harmonic generation in roughly the same parameter region.

Following the ideas of the much simpler problem of a single small Josephson junction discussed in Ref. 11, we assume a solution for the in-phase mode ($\phi = \phi_{10} = \phi_{21}$)

$$\phi = \phi_0 + \phi_1 \cos(\Omega t - Kx - \theta) + \delta\phi, \tag{3}$$

where we assume $\phi_1 \ll 1$ and $\delta\phi \ll 1$. For the components at dc, ϕ_0, and at frequency Ω, ϕ_1, we get $\sin \phi_0 \cong \eta_0$ and

$$\phi_1 = \eta_{\mathrm{rf}} / \{(K^2\Gamma^2 - \Omega^2 + \cos\phi_0)^2 + \alpha^2\Omega^2\}^{1/2} \tag{4}$$

with $\tan\theta = \alpha\Omega/(K^2\Gamma^2 - \Omega^2 + \cos\phi_0)$. Equation (4) has (in unnormalized units, i.e., $\omega = \Omega\omega_0$ and $k = K/\lambda_J^{(1)}$) a resonance at

$$\omega^2 = \omega_0^2 \cos\phi_0 + (c^{(2)})^2 k^2, \tag{5}$$

i.e., at the plasma resonance for the in-phase mode as discussed in Ref. 8.

The equation for $\delta\phi$ (i.e., the remaining terms not at dc or ω) may be linearized to the form

$$\delta\phi_{xx}\Gamma^2 + \delta\phi_{tt} + \alpha\,\delta\phi_t + \cos\phi_0[1 - \phi_1 \tan\phi_0 \times \cos(\Omega t - Kx - \theta)]\,\delta\phi = F(\Omega t). \tag{6}$$

Following the methods from Ref. 11 the particular solution to the inhomogeneous equation may be disregarded, only the full solution to the homogeneous equation obtained by setting $F(\Omega t) = 0$ is important. Following again Ref. 11 we introduce the substitutions

$$\delta\phi = e^{-az/2} \cdot \delta\phi' \tag{7}$$

and

$$2z = \Omega t - Kx - \theta, \tag{8}$$

and obtain the Mathieu equation[12]

$$\delta\phi'_{zz} + [a - 2q\cos(2z)]\,\delta\phi' = 0, \tag{9}$$

where

$$a = \frac{4\omega_0^2 \cos\phi_0}{\omega^2 - (c^{(2)}k)^2}\left[1 - \left(\frac{1}{2Q}\right)^2\right] \tag{10a}$$

and

$$2q = \frac{4\omega_0^2 \cos\phi_0}{\omega^2 - (c^{(2)}k)^2}\,\phi_1 \tan\phi_0 \tag{10b}$$

with $Q = \sqrt{\cos\phi_0}/\alpha = \omega_0\sqrt{\cos\phi_0}RC$. The only difference between Eqs. (10) and the results from Ref. 11 is the k^2 term in the denominator. The possible values of k are related to factors such as the length of the junction and the applied magnetic field and will be discussed below.

The solutions to the Mathieu equation, Eq. (9), gives rise to the fundamental half harmonic generation subject to the condition $a = 1$. In the limit $(Q \gg 1)$ this may be expressed as

$$\omega^2 = (2\omega_0\sqrt{\cos\phi_0})^2 + (c^{(2)}k)^2 \tag{11}$$

and

$$\phi_1 \tan\phi_0 > 2/Q.$$

Without the k^2 term, Eq. (11) just gives the well-known condition for half harmonic generation[11] in a small Josephson junction, when the applied frequency is twice the plasma frequency $\omega_0\sqrt{\cos\phi_0}$ and the applied rf amplitude is sufficiently large.

For the case investigated here the rf voltages not only have a frequency dependence with a (plasma) resonance, but also a spatial dependence with a geometric resonance. The fundamental, symmetric spatial resonance has $k = 2\pi/l$ where l is the unnormalized length of the junction.

In general a symmetric spatial excitation will contain the fundamental spatial component $k_0 = 2\pi/l$ and higher harmonics. With an applied magnetic field or a spatially nonsymmetric current, nonsymmetric components with $k = k_0/2$ will also appear. We will not consider this case here, although a simple extension of our calculation can be made.

Since from Eqs. (2) and (8) both time and space appear we will expect the half harmonic generation to occur at the spatial resonance with $k_0 = 2\pi/l$. Since the independent variable in the Mathieu equation is defined by $2z = \Omega t - Kx - \theta$ the fundamental spatial resonance is exited from a spatial component with $k' = 2k_0 = 4\pi/l$. Inserting this in Eq. (11) we obtain the resonance condition for half harmonic generation in time and space

$$\omega^2 = 4(\omega_0\sqrt{\cos\phi_0})^2 + 4(c^{(2)}k)^2 \tag{12}$$

with $k = 2\pi/l$ or equivalently $\omega^2 = (2\omega_p)^2$, where ω_p is the two-junction in-phase plasma frequency[8] defined by Eq. (5).

In addition to Eq. (12), a threshold in the external rf power must be exceded [the second condition in Eq. (11)]. In our derivation above, the treatment of the time dependence was more complete than that of the space dependence. We note, however, that by including a full treatment of the spatial resonances[13] the same results could have been obtained in a formally more correct way. We have not done that in order to preserve clarity.

We note that our results obtained for the in-phase mode with $N = 2$ can be generalized to $N = 1$ by assuming $\Gamma = 1$ in Eq. (2). We may also utilize the results of Ref. 8 to the case

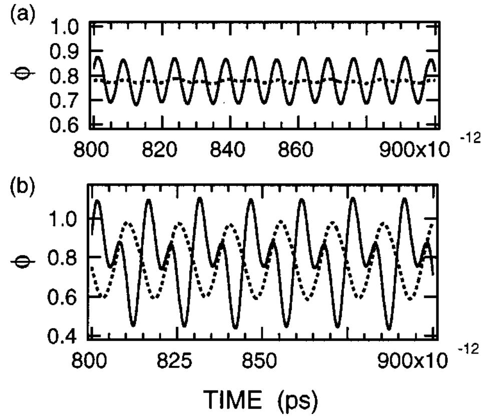

FIG. 2. ϕ_{10} and ϕ_{21} as a function of time at $\Omega=2.48$. ϕ_{10} and ϕ_{21} are perfectly identical with each other ($\phi_{10}=\phi_{21}=\phi$). (a) $\eta_{\rm rf}=0.6$ and (b) $\eta_{\rm rf}=1.2$. The solid curve shows the ϕ variation at the center of the junctions 1 and 2, and the dotted curve is the ϕ variation at the edge of the junctions 1 and 2.

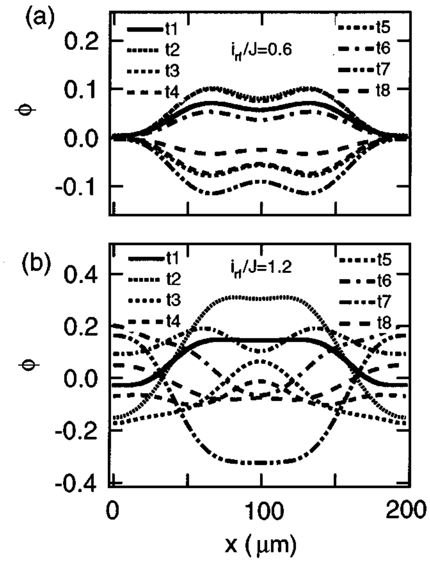

FIG. 3. Spatial dependence corresponding to Fig. 2. (a) $\eta_{\rm rf}=0.6$ and (b) $\eta_{\rm rf}=1.2$. Here ϕ_0 is subtracted from all curves.

of the large Josephson stack ($N \gg 1$) in-phase plasma mode. For this case we must use $\Gamma^2=\Gamma_\infty^2=(\lambda_J^\infty/\lambda_J^{(1)})^2=d'/(d'+2s)$. We assume—supported by numerical simulations—that the parametric half harmonic generation for the in-phase plasma mode may take place for arbitrary N. Indeed, for $N=3$ we found numerically half harmonic generation although the voltage amplitude of the middle junction is not the same as the top and bottom junctions.[14]

The obtained analytical results have been tested in numerical simulations. In our simulations we have assumed a standing wave for the applied rf signal instead of a traveling wave. We note that the standing wave is the result of having a superposition of two waves with positive and negative k. Thus in our simulation we have assumed

$$\eta=\eta_0+\eta_{\rm rf}\sin(Kx)\cos(\Omega t) \tag{13}$$

with

$$K=(\pi/l)\lambda_J^{(1)} \quad \text{and} \quad 0\leqslant x\leqslant l/\lambda_J^{(1)}.$$

We suspect that we could have introduced the necessary k dependence by having a nonuniform dc bias instead. This would have introduced the necessary spatial components.[15]

The calculations were typically done in real units with parameters corresponding to either low T_c niobium-type stacks or to high-T_c BSCCO-type stacks. Thus in Fig. 2 the parameters are $l=200\,\mu$m, $\eta_0=0.7$, the coupling factor $S\equiv s/d'=-0.79$, $RC=1\times10^{10}$ s, and $N=2$, leading to $\omega_0=337\times10^9$ rad/s, $\omega_0\sqrt{\cos\phi_0}=285\times10^9$ rad/s, $kc^{(2)}=305\times10^9$ rad/s at $k=2\pi/l$, $\omega_p=417\times10^9$ rad/s, i.e., $\omega_p/\omega_0=1.24$, and $Q\cong30$.

In Fig. 2 we show for the drive frequency equal to twice the plasma frequency [Eq. (12)], i.e., $\Omega=2.48$, the time dependence of ϕ for the in-phase mode ($\phi=\phi_{10}=\phi_{21}$) in the center and at the edge of the junctions. Figure 2(a) shows a case just below threshold ($\eta_{\rm rf}=0.6$) and Fig. 2(b) shows the case above threshold ($\eta_{\rm rf}=1.2$). We note that the half harmonic generation is clearly visible. We also note that the simple threshold condition in Eq. (11), $\phi_1\tan\phi_0>2/Q$, in principle cannot be used directly, since the applied rf signal and the rf voltage varies over the junction. Nevertheless in the numerical simulation we can make an estimated spatial average of ϕ_1. For Fig. 2(b) we find $\phi_1\approx0.1$, in rough agreement with the threshold condition in Eq. (11). Also the smallness condition $\phi_1\ll1$ from Eq. (3) is clearly satisfied. Because of the basic properties of the Mathieu equation, giving exponentially growing solutions in time and space above the threshold, the other smallness condition in Eq. (3), $\delta\phi\ll1$, is not satisfied above threshold, only below and just below.[11,12]

We also note from Fig. 2(b) that at the junction edge, the generated half harmonic component is completely dominant, while at the center, a component of the external drive frequency may still be seen. The reason for this may be understood again from the basic properties of the Mathieu equation. Above threshold spatial excitations of the form e^{kx}, which is most dominant at the edge, will appear. The spatial pattern of the phase (or equivalently the rf voltage) is of course complicated, and we will not discuss the details here. Figure 3 shows, however, an example of the spatial patterns corresponding to the situations below and above threshold as shown in Fig. 2. The parameters are those of Fig. 2, and the curves correspond to different times during a period of the external drive (the traces are shown for 2 ps time intervals). We notice from Fig. 3(b)—in accordance with the prediction of the Mathieu equation—the strong appearance of the half-harmonic spatial component, when compared to Fig. 3(a).

The parameters used in the simulation correspond to identical junctions. We have tried to vary the parameters to have dissimilar junctions in the stack (typically 10% difference). We found that the half harmonic generation was rather insensitive to such a change. This is, of course, important for an experimental confirmation. In low-T_c niobium stacks and in bulk BSCCO single crystals a 10% difference should be realistic. In BSCCO thin films the spread may be larger.

We further note that the spatial dependence of the phase is essential, as was also found for the plasma resonance.[8] If we assume a uniform rf drive in Eq. (13), half harmonic generation at the plasma resonance, such as that shown in Figs. 2 and 3, is not observed. Only at $\Omega=1.69$,($\eta_{\rm rf}=0.4$) corre-

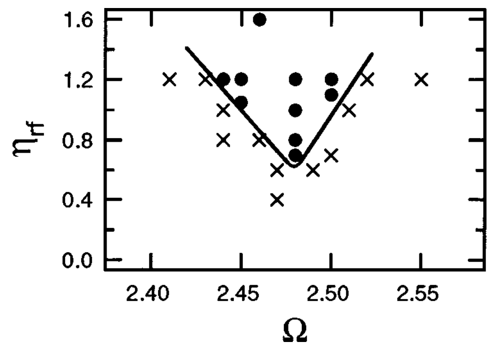

FIG. 4. Region of half harmonic generation at the plasma resonance in the Ω versus η_{rf} plane. Parameters correspond to those of Fig. 2.

sponding to the well known $k=0$ case[11] for small junctions, half harmonic generation may be observed.

Finally, Fig. 4 shows the threshold region in the Ω versus η_{rf} plane for half harmonic excitation at the in-phase stack plasma resonance defined in Eq. (5). We note the threshold region is in full qualitative agreement with Eqs. (12) and (13) and rather similar to that of Ref. 11.

Excitations corresponding to higher order excitations of the Mathieu equation are expected to also exist in Josephson stacks. The mixture of spatial and frequency resonances may also give rise to new modes. Likewise it is possible that other plasma resonance modes than the in-phase modes may show a similar behavior, but we estimate that analytic results for this case are much more difficult to obtain than for the in-phase modes.

We have demonstrated analytically and numerically the existence of half harmonic excitations in stacked Josephson junctions. The phenomenon could offer a possibility to make high-frequency (hundreds of Gigahertz) electronic components employing the Josephson effect in high-T_c single crystals of the BSCCO type. At the same time the phenomenon and its extension to higher-order modes has some nonlinear features with coexisting time and space excitations. Extension of our work to other plasma modes and higher drive levels is likely to reveal a whole new world of space-time nonlinear excitations.

[1] K. C. Tsui *et al.*, Phys. Rev. Lett. **73**, 724 (1994).
[2] M. Tachiki, T. Koyama, and S. Takahashi, Phys. Rev. B **50**, 7065 (1994).
[3] L. N. Bulaevskii, V. L. Pokrovsky, and M. P. Maley, Phys. Rev. Lett. **76**, 1719 (1996).
[4] Y. Matsuda *et al.*, Phys. Rev. Lett. **78**, 1972 (1997).
[5] M. Tachiki, *et al.*, in *Coherence in High Temperature Superconductors*, edited by G. Deutsher and A. Revolevschi (World Scientific, Singapore, 1996), p. 371.
[6] T. Koyama and M. Tachiki, Phys. Rev. B **54**, 16 183 (1996).
[7] I. Kakeya *et al.*, Phys. Rev. B **57**, 3108 (1998).
[8] N. F. Pedersen and S. Sakai, Phys. Rev. B **58**, 2820 (1998).
[9] S. Sakai and N. F. Pedersen, Phys. Rev. B **60**, 9810 (1999).
[10] S. Sakai, P. Bodin, and N. F. Pedersen, J. Appl. Phys. **73**, 2411 (1993).
[11] N. F. Pedersen, M. R. Samuelsen, and K. Saermark, J. Appl. Phys. **44**, 5120 (1973).
[12] M. Abramowitz and I. A. Stegun, *Handbook of Mathematical Functions* (Dover, New York, 1965).
[13] M. Cirillo *et al.*, Phys. Rev. B **58**, 12 377 (1998).
[14] S. Sakai and N. F. Pedersen (unpublished).
[15] G. Filatrella and N. F. Pedersen, J. Appl. Phys. **85**, 6904 (1999).